


Biomimetic Multifunctional Porous Chalcogels as Solar Fuel Catalysts

Benjamin D. Yuhas,[†] Amanda L. Smeigh,[†] Amanda P. S. Samuel,[†] Yurina Shim,[†] Santanu Bag,[†] Alexios P. Douvalis,[‡] Michael R. Wasielewski,[†] and Mercuri G. Kanatzidis^{*,†,§}

[†]Department of Chemistry and Argonne–Northwestern Solar Energy Research (ANSER) Center, Northwestern University, Evanston, Illinois 60208-3113, United States

[‡]Department of Physics, University of Ioannina, 45110 Ioannina, Greece

[§]Materials Science Division, Argonne National Laboratory, Argonne, Illinois 60439, United States

 Supporting Information

ABSTRACT: Biological systems that can capture and store solar energy are rich in a variety of chemical functionalities, incorporating light-harvesting components, electron-transfer cofactors, and redox-active catalysts into one supramolecule. Any artificial mimic of such systems designed for solar fuels production will require the integration of complex subunits into a larger architecture. We present porous chalcogenide frameworks that can contain both immobilized redox-active Fe₄S₄ clusters and light-harvesting photoredox dye molecules in close proximity. These multifunctional gels are shown to electrocatalytically reduce protons and carbon disulfide. In addition, incorporation of a photoredox agent into the chalcogels is shown to photochemically produce hydrogen. The gels have a high degree of synthetic flexibility, which should allow for a wide range of light-driven processes relevant to the production of solar fuels.

The quest for renewable energy production from sunlight has led to an intense research effort in the field of solar fuels. Many approaches have focused on mimicking naturally occurring processes such as photosynthesis,¹ where light-driven water splitting by the Photosystem II reaction center protein yields both oxygen and protons. In contrast, biological proton reduction to hydrogen is catalyzed by hydrogenases that generally occur in non-photosynthetic organisms, and recent research on these enzymes largely focuses on their hydrogen-producing capabilities,² particularly as a function of different environments, such as one might encounter in nature³ or in a purely engineered design,⁴ with an applied electrochemical or photochemical potential driving the generation of hydrogen from protons.

Using proteins and other biological structures as starting points, researchers have developed analogous inorganic and organometallic molecules that can catalyze hydrogen production from water.⁵ Many of these compounds have been shown to be reasonably successful at short-term hydrogen production,⁶ yet the major limitation of these molecules arises from catalyst deactivation, primarily by oxygen, which is both the other product of the water-splitting reaction and a major component of the atmosphere. It is clear, then, that any design motif that incorporates active catalysts into a larger framework that can serve to protect the catalysts from the adverse effects of oxygen may significantly improve long-term catalyst stability.

A newly emerging class of porous chalcogenide aerogels, or “chalcogels”, may be an ideal supramolecular structure for the integration of redox-active cofactors relevant to solar fuels production.⁷ Chalcogels are highly porous materials that, unlike the ubiquitous oxide-based aerogels,⁸ are based on chalcogenide materials such as sulfides, selenides, and tellurides. This allows for the possibility of strong visible light absorption, as well as a number of other interesting properties, such as desulfurization catalysis⁹ and heavy metal ion sequestration.⁷

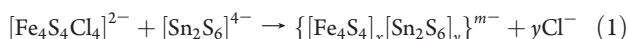
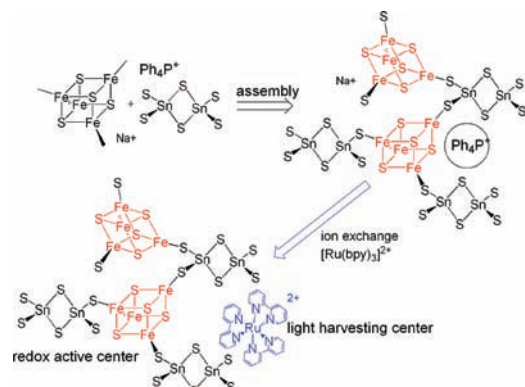
Here, we present a new type of chalcogel that contains both redox-active transition metal clusters and light-harvesting photoredox molecules. The transition metal clusters are Fe₄S₄ cubane clusters that are known redox-active cofactors in enzymes. Synthetic molecular analogues of these bioinorganic Fe₄S₄ cofactors have existed for some time.¹⁰ We show that the Fe₄S₄ cubane clusters retain their redox activity when incorporated into a larger chalcogenide gel framework and that their redox states can be switched electrochemically. We also demonstrate the catalytic potential of these Fe₄S₄-functionalized chalcogels through electrocatalytic reduction of protons, provided by the weak organic acid lutidinium, and carbon disulfide (CS₂), a more-readily reduced surrogate for CO₂. Finally, we show that cationic light-harvesting photoredox dyes can be incorporated into the chalcogel framework by a simple ion-exchange process, that the excited states of these photoredox dye molecules are strongly quenched by the presence of the Fe₄S₄ cubane clusters in the gels, and that the dye-functionalized gels are capable of photochemically producing hydrogen. The chalcogels are multifunctional materials with high porosity that can be engineered and functionalized to have all of the components required for light-driven chemical catalysis, providing new integrated materials for solar fuels production.

The slow, controlled metathesis reaction between the precursors Na₄Sn₂S₆·14H₂O and (Ph₄P)₂[Fe₄S₄Cl₄] results in replacement of the terminal chloride ligands on the iron–sulfur cubane cluster with sulfur atoms from the tin sulfide cluster (Scheme 1), giving a polymerized network that condenses in a solid, spongy gel (Figure 1A,B). Electron microscopy reveals the spongy, porous nature of these chalcogels, which always appear amorphous under TEM as well as in capillary X-ray diffraction experiments. With multiple binding points on each Fe₄S₄ cluster, the reaction can occur at up to four points per cluster, as suggested by the equation

Received: December 23, 2010

Published: March 16, 2011

Scheme 1. Reaction between $[\text{Sn}_2\text{S}_6]^{4-}$ and $[\text{Fe}_4\text{S}_4\text{Cl}_4]^{2-}$ Cluster Anions and Functionalization of the Framework with Light-Harvesting $\text{Ru}(\text{bpy})_3^{2+}$



The porous structures are formed without the use of templating agents. The pore sizes and porosity can be described as a mixture of macroporous and mesoporous structures, as evidenced by the nitrogen adsorption isotherms (Figure 1C), which exhibit Type IIb behavior.¹¹ The resulting estimated surface areas range from 90 to 290 m²/g. Elemental analysis (Figure 1D) of the chalcogels consistently shows, in addition to all of the expected elements, signatures arising from the counter-cations of the precursors, Ph_4P^+ and Na^+ . This indicates that the chalcogel network is overall negatively charged ($\{[\text{Fe}_4\text{S}_4]_x[\text{Sn}_2\text{S}_6]_y\}^{m-}$, eq 1 and Scheme 1). The remaining charge is balanced by either Ph_4P^+ or Na^+ .

Characterization of the Fe/S clusters inside the chalcogels was accomplished by UV-vis and Mössbauer spectroscopies. Although the chalcogels are stable in nearly all solvents with no observable leaching, when a large excess of benzenethiol is added to the solution, the thiol extrudes the Fe/S clusters from the gel framework, and eventually a uniform solution results. The characteristic UV-vis spectra in *N,N'*-dimethylformamide (DMF) are shown in Figure 1F, with the well-known¹² absorption maximum of $[\text{Fe}_4\text{S}_4(\text{SPh})_4]^{2-}$ appearing at ~ 460 nm. This is also a well-established method of detecting Fe_4S_4 clusters in their native proteins.¹³

Figure 1G,H shows zero-field ⁵⁷Fe Mössbauer spectra acquired at 40 and 10 K, respectively. At 40 K, the spectrum is characterized by two very closely spaced quadrupole doublets, suggesting a high degree of equivalence among the Fe centers of the clusters in the gels. The isomer shifts (δ) of the two doublets are found to be 0.49 and 0.47 mm/s (relative to α -Fe), with respective quadrupole splitting parameters (ΔE_{q}) of 1.07 and 0.66 mm/s. This finding is consistent with previous Mössbauer investigations on isolated, molecular analogues of the Fe_4S_4 cluster,¹⁴ as well as on native Fe_4S_4 -bearing proteins, such as ferredoxins.¹⁵ At 10 K, however, we begin to observe a magnetic hyperfine splitting of the Mössbauer signal, despite the absence of an applied magnetic field. This could be the effect of a residual paramagnetic state in the gels, or perhaps the effect of *intercluster* coupling within the chalcogels. In native proteins, the Fe_4S_4 cubane moiety is sometimes found in chains to facilitate electron transfer, such as in bacterial ferredoxins.¹⁵ However, to our knowledge, no zero-field Mössbauer magnetic splitting has been reported in systems

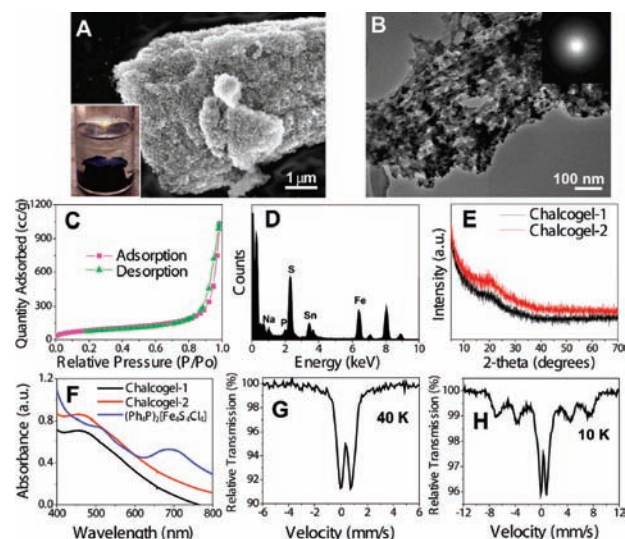


Figure 1. (A,B) SEM and TEM images of a typical Fe_4S_4 - Sn_2S_6 chalcogel. Insets: (A) real-size image of the chalcogel; (B) representative SAED pattern of the chalcogels. (C) Nitrogen adsorption/desorption isotherm at 77 K of the chalcogel. (D) Typical EDS spectrum of the chalcogels. (E) XRD patterns of the chalcogels, illustrating their amorphous character. (F) UV-vis spectra of DMF solutions of chalcogels that have been exposed to excess benzenethiol, reflecting the absorption of the extruded $[\text{Fe}_4\text{S}_4(\text{SPh})_4]^{2-}$ anion. The spectrum of the precursor $(\text{Ph}_4\text{P})_2[\text{Fe}_4\text{S}_4\text{Cl}_4]$ is included for comparison. (G,H) Mössbauer spectra of Chalcogel-1 at 40 and 10 K.

containing multiple Fe_4S_4 clusters. Nevertheless, it should be noted that the possibility exists for the two or more Fe_4S_4 clusters to be in very close proximity (i.e., separated by a single $[\text{Sn}_2\text{S}_6]^{4-}$ unit), which could enable intercluster coupling.

The chalcogels' Fe_4S_4 cluster redox activity was examined with cyclic voltammetry (Figure 2). All CV experiments were performed on the chalcogels in the solid state. Sweeping the potential in a reductive direction revealed an initial reduction near -800 to -900 mV (vs Ag/AgCl) and a second event further negative, near -1500 to -1600 mV. The redox potentials of the Fe_4S_4 cubane clusters *in solution* have been well-studied,¹² but there are comparatively fewer literature reports on the redox activity of these types of clusters in bound environments,¹⁶ aside from the native proteins themselves. The first reduction at -900 mV is assigned to $[\text{Fe}_4\text{S}_4]^{2+/\cdot+}$ core cluster reduction. The potential at which this occurs is in good agreement with previous studies in solution. While the first reduction wave exhibits reversible behavior in many of these solution-based studies, in our case the reduction is decidedly quasi-reversible, if not irreversible. Upon reversing the direction of the scan, an anodic wave is observed at least 600 mV more positive than the initial reduction wave. This large separation between the initial reduction and subsequent re-oxidation waves is nearly unprecedented and suggests either a capacitive effect in the gel or perhaps a charge transfer into the gel backbone. Furthermore, we observe that there is little to no dependence of the CV curves on solvent, electrolyte, or scan rate. This suggests that what we are measuring is due entirely to the solid gel on the surface of the electrode and is not a result of Fe_4S_4 clusters leaching into the electrolyte solution. The second observed reduction wave could be attributed to the $[\text{Fe}_4\text{S}_4]^{+/0}$ reduction. In solution, this reduction is always irreversible.¹⁷ However, the all-ferrous state of the cluster could be more easily stabilized when bound in the chalcogel. When the gels are prepared without Fe_4S_4 clusters, we see no comparable redox events (Figure 2B).

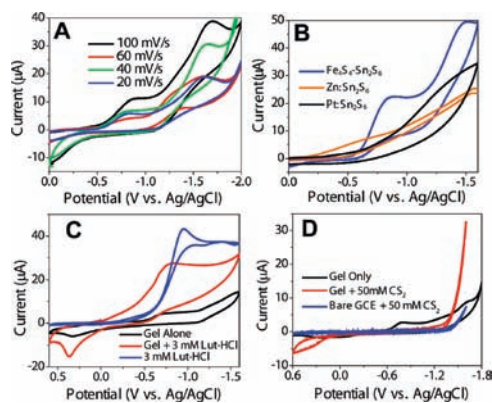


Figure 2. (A) CVs of $\text{Fe}_4\text{S}_4\text{-Sn}_2\text{S}_6$ chalcogel at varying scan rates. (B) Various chalcogel CVs scanned at 100 mV/s. Only the chalcogels synthesized with the Fe_4S_4 clusters exhibit redox activity. (C,D) CVs of chalcogels with lutidinium chloride (C) and CS_2 (D) as substrates dissolved in solution. The scan rate is 20 mV/s in each case.

The reproducible redox activity of these Fe_4S_4 -containing chalcogels coupled with their high degree of porosity make them excellent electrocatalyst candidates. We explored this possibility by probing the electrochemical reduction of two substrates, lutidinium ion and CS_2 , in the presence of the chalcogel-modified electrodes. Lutidinium was chosen because isolated Fe_4S_4 clusters in solution have been shown to reduce protons from weak organic acids such as lutidinium, pyridinium, and other similar sources,¹⁸ whereas CS_2 was examined as a more easily reduced analogue of CO_2 , which has also been shown to undergo enhanced electrochemical reduction in the presence of artificial Fe_4S_4 -bearing molecules.¹⁹ The latter experiments involved free, isolated clusters in solution, not bound into a larger supramolecular framework as is the case in our chalcogels.

Figure 2C shows the CVs for electrochemical reduction of lutidinium cations in acetonitrile in the presence and absence of $\text{Fe}_4\text{S}_4\text{-Sn}_2\text{S}_6$ chalcogels. A modest, ~ 6 -fold increase in current of the reduction wave is seen when the chalcogel is present on the working electrode, as compared to when no lutidinium is present in the electrolyte. Additionally, there is a clear shift in the potential (~ 200 mV) at which reduction occurs when the chalcogel is present as opposed to a bare working electrode. A similar set of experiments is presented in Figure 2D, this time using CS_2 as the substrate in DMF. In this case, the ~ 10 -fold current increase with the chalcogel present is greater than that observed in the lutidinium experiments. There is also an anodic shift in the potential at which the current begins to rise rapidly (~ 200 mV). Further experiments with these and other substrates are ongoing, but our results suggest that the chalcogels could be effective electrocatalysts for the reduction of substrates relevant to solar fuels.

As mentioned above, elemental analysis of the fully washed chalcogels always reveals a persistent quantity of the counter-cation associated with the chalcogel precursors. This indicates that the metal sulfide framework is anionic, which allows for the possibility for ion-exchange, specifically the exchange of the counter-cations such as light-harvesting photoredox dyes. Thus, to examine photodriven electron-transfer chemistry and potential photocatalysis in chalcogels, we functionalized chalcogels with $\text{Ru}(\text{bpy})_3^{2+}$. Solution-based ion exchange results in the dye molecules displacing the existing cations (Na^+ and Ph_4P^+) and remaining electrostatically bound to the chalcogel surface. Dye functionalization is confirmed by FTIR and EDS spectroscopy

(Supporting Information (SI), Figure S1). No leaching of the dyes was observed. The dye-functionalized gels are placed in *o*-dichlorobenzene and sonicated, resulting in a thick slurry that is spun onto a glass substrate to give thin films of the gels.

The $\text{Ru}(\text{bpy})_3^{2+}$ -functionalized films were then examined by transient absorption spectroscopy (for full details, see the SI). All of the samples show a clear bleaching of the ground state at 460 nm, and both gel samples exhibit multiphasic recovery of the $\text{Ru}(\text{bpy})_3^{2+}$ ground-state bleach. However, the amount of residual bleach remaining on a sub-nanosecond time scale is significantly larger in the $\text{Zn:Sn}_2\text{S}_6$ control gel than in the $\text{Fe}_4\text{S}_4\text{:Sn}_2\text{S}_6$ gel (48% and 11%, respectively). In the $\text{Ru}(\text{bpy})_3^{2+}$ -functionalized $\text{Fe}_4\text{S}_4\text{:Sn}_2\text{S}_6$ gels, nearly 90% of the excited state is quenched within a few picoseconds. This stands in stark contrast to $\text{Ru}(\text{bpy})_3^{2+}$ in solution, which exhibits essentially zero decay of the excited state on the time scale of interest because of its intrinsic 600 ns excited-state lifetime. Figure 3A shows the decay of the ground-state bleach at 460 nm of $\text{Ru}(\text{bpy})_3^{2+}$ in both the $\text{Fe}_4\text{S}_4\text{:Sn}_2\text{S}_6$ and $\text{Zn:Sn}_2\text{S}_6$ gels, as well as $\text{Ru}(\text{bpy})_3^{2+}$ in solution. The rapid decay at 460 nm, on the <10 ps time scale, indicates an additional deactivation pathway is present in the $\text{Fe}_4\text{S}_4\text{:Sn}_2\text{S}_6$ gel, which is absent in the $\text{Zn:Sn}_2\text{S}_6$ gel. The residual, unquenched signal in the $\text{Zn:Sn}_2\text{S}_6$ gel is likely associated with the $\text{Ru}(\text{bpy})_3^{2+}$ excited state, as evidenced by nanosecond transient absorption measurements (SI, Figure S2). On the nanosecond time scale, an emissive feature at 620 nm is observed in both solution and the control $\text{Zn:Sn}_2\text{S}_6$ gel but is absent in the $\text{Fe}_4\text{S}_4\text{:Sn}_2\text{S}_6$ gel.

The exact mechanism of excited-state quenching is still under investigation. Since we cannot observe any distinguishing spectroscopic features of $\text{Ru}(\text{bpy})_3^{3+}$ or $\text{Ru}(\text{bpy})_3^+$, it is difficult to say if quenching occurs primarily by oxidative or reductive pathways. However, the possibility of oxidative quenching of $\text{Ru}(\text{bpy})_3^{2+}$ by the Fe_4S_4 cluster is supported by an approximate calculation of the free energy for photodriven electron transfer from the photogenerated metal-to-ligand charge-transfer state of $\text{Ru}(\text{bpy})_3^{2+}$ to the Fe_4S_4 cluster using the Weller equation,²⁰ which gives a favorable free energy change for this process of about $\Delta G = -90$ meV. The proposed energy level diagram, constructed from the electrochemical and photophysical measurements, is shown in Figure 3B. Although ΔG is small, the Coulombic attraction between the anionic, anchored Fe_4S_4 clusters and the cationic $\text{Ru}(\text{bpy})_3^{2+}$ photoredox dye means that we expect these two functional groups to be positioned very close to each other, which should facilitate electron transfer by increasing the electronic coupling between them.

As a practical demonstration of the potential photocatalytic capability of our photoredox dye-functionalized chalcogels, photochemical hydrogen evolution experiments were performed (Figure 3C). The solid $\text{Ru}(\text{bpy})_3^{2+}$ -functionalized gels were placed in an acetonitrile/water (70:30 v/v) solution containing 50 mM lutidinium chloride and 50 mM sodium ascorbate as a sacrificial electron donor and then continuously irradiated with a xenon lamp ($\lambda > 300$ nm). After 24 h, H_2 gas was detected by gas chromatography, and the amount of H_2 produced increased steadily over 4 days of illumination. There was no detectable H_2 evolution when the dye-functionalized gels were kept in darkness or when a gel-free solution containing lutidine, ascorbate, and $\text{Ru}(\text{bpy})_3^{2+}$ was illuminated. Irradiation of control gels lacking $\text{Ru}(\text{bpy})_3^{2+}$ produced only a very small amount of H_2 that only was observable above the baseline after about 2 days. The amount of H_2 produced by the dye-functionalized gels was about 8-fold greater than that generated by gels with no photoredox dye present. Further

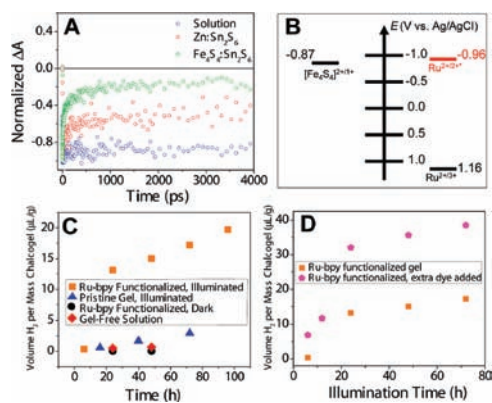


Figure 3. (A) Femtosecond transient absorption at 460 nm of Ru(bpy)₃²⁺ dye in three different environments: free in solution, in a control Zn:Sn₂S₆ gel, and in the redox-active Fe₄S₄–Sn₂S₆ gel. Within a few picoseconds, almost 90% of the excited state is quenched by the Fe₄S₄ clusters. (B) Proposed energy diagram for the Ru(bpy)₃²⁺ dye in the Fe₄S₄–Sn₂S₆ chalcogels, as calculated from cyclic voltammetry and spectroscopic experiments. (C) Hydrogen evolution for a variety of gels and conditions. The volume of H₂ evolved is normalized to the dry mass of the chalcogels, where applicable. (D) Hydrogen evolution of Ru(bpy)₃²⁺-functionalized gels, showing the beneficial effect of adding extra dye (100 mM) into the solution.

enhancement of the H₂ output is observed when extra Ru(bpy)₃²⁺ is dissolved in the gel-containing solutions with the lutidinium and ascorbate (Figure 3D). Although the overall H₂ output is rather small (~0.2 mol % based on [Fe₄S₄]), it is reasonable to envision that through further optimization, such as manipulation of the reduction potentials of the clusters and/or the photoredox dyes, photochemical H₂ production could be greatly enhanced.

The chalcogel system presented here allows us to fabricate multifunctional and chemically integrated materials using a relatively facile synthetic method. We have shown that porous frameworks with controllable and tunable light absorption can be made to include both redox-active components important to catalysis and light-harvesting photoredox components necessary for solar energy conversion. The presence of the biomimetic redox-active clusters in the gels not only facilitates electrochemical reductions of various substrates but also provides a means of positioning photoredox molecules sufficiently close to the redox-active Fe₄S₄ clusters to promote rapid excited-state quenching of the photoredox dye excited states. The photoredox dye-functionalized gels are capable of producing hydrogen under photochemical conditions. The chalcogels have the distinct advantage of being easy to scale up as well as providing spatial separation between active redox groups. This could ultimately lead to a self-assembling, fully synthetic material that encompasses and emulates all of the active materials of biological systems involved in solar energy conversion.

■ ASSOCIATED CONTENT

Supporting Information. Experimental and characterization details and spectra. This material is available free of charge via the Internet at <http://pubs.acs.org>.

■ AUTHOR INFORMATION

Corresponding Author
m-kanatzidis@northwestern.edu

■ ACKNOWLEDGMENT

We thank Prof. Joseph Hupp for use of the potentiostat. Electron microscopy and elemental analysis were performed at the Electron Probe Instrumentation Center at Northwestern University. This work was supported as part of the ANSER Center, an Energy Frontier Research Center funded by the U.S. Department of Energy, Office of Science, Office of Basic Energy Sciences, under Award No. DE-SC0001059.

■ REFERENCES

- (1) (a) Ferreira, K. N.; Iverson, T. M.; Maghlaoui, K.; Barber, J.; Iwata, S. *Science* **2004**, *303*, 1831. (b) Youngblood, W. J.; Lee, S.-H. A.; Maeda, K.; Mallouk, T. E. *Acc. Chem. Res.* **2009**, *42*, 1966. (c) Gust, D.; Moore, T. A.; Moore, A. L. *Acc. Chem. Res.* **2009**, *42*, 1890.
- (2) Vincent, K. A.; Parkin, A.; Armstrong, F. A. *Chem. Rev.* **2007**, *107*, 4366.
- (3) (a) Ihara, M.; Nishihara, H.; Yoon, K.-S.; Lenz, O.; Friedrich, B.; Nakamoto, H.; Kojima, K.; Honma, D.; Kamachi, T.; Okura, I. *Photochem. Photobiol.* **2006**, *82*, 676. (b) Fouchard, S.; Hemschemeier, A.; Caruana, A.; Pruvost, J.; Legrand, J.; Happe, T.; Peltier, G.; Cournac, L. *Appl. Environ. Microbiol.* **2005**, *71*, 6199.
- (4) (a) Dementin, S.; Belle, V.; Guigliarelli, B.; Adryanczyk-Perrier, G.; De Lacey, A. L.; Fernandez, V. M.; Rousset, M.; Leger, C. *J. Am. Chem. Soc.* **2006**, *128*, S209. (b) Jones, A. K.; Sillery, E.; Albracht, S. P. J.; Armstrong, F. A. *J. Chem. Soc., Chem. Commun.* **2002**, 866.
- (5) (a) Tard, C.; Liu, X.; Ibrahim, S. K.; Bruschi, M.; De Gioia, L.; Davies, S. C.; Yang, X.; Wang, L.-S.; Sawers, G.; Pickett, C. J. *Nature* **2005**, *433*, 610. (b) Schmidt, M.; Contakes, S. M.; Rauchfuss, T. B. *J. Am. Chem. Soc.* **1999**, *121*, 9736. (c) Evans, D. J.; Pickett, C. J. *Chem. Rev.* **2003**, *32*, 268.
- (6) (a) Gloaguen, F.; Lawrence, J. D.; Rauchfuss, T. B. *J. Am. Chem. Soc.* **2001**, *123*, 9476. (b) Christou, G.; Hageman, R. V.; Holm, R. H. *J. Am. Chem. Soc.* **1980**, *102*, 7600.
- (7) Bag, S.; Trikalitis, P. N.; Chupas, P. J.; Armatas, G. S.; Kanatzidis, M. G. *Science* **2007**, *317*, 490.
- (8) Husing, N.; Schubert, U. *Angew. Chem., Int. Ed.* **1998**, *37*, 22.
- (9) Bag, S.; Gaudette, A. F.; Bussell, M. E.; Kanatzidis, M. G. *Nat. Chem.* **2009**, *1*, 217.
- (10) Rao, P. V.; Holm, R. H. *Chem. Rev.* **2004**, *104*, 527.
- (11) Sing, K. S. W.; Everett, D. H.; Haul, R. A. W.; Moscou, L.; Pierotti, R. A.; Rouquerol, J.; Siemieniwska, T. *Pure Appl. Chem.* **1985**, *57*, 603.
- (12) (a) Coucouvanis, D.; Kanatzidis, M. G.; Simhon, E.; Baenziger, N. C. *J. Am. Chem. Soc.* **1982**, *104*, 1874. (b) Wong, G. B.; Bobrik, M. A.; Holm, R. H. *Inorg. Chem.* **1978**, *17*, 578.
- (13) Moulis, J. M.; Meyer, J. *Biochemistry* **1982**, *21*, 4762.
- (14) (a) Holm, R. H.; Averill, B. A.; Herskovitz, T.; Frankel, R. B.; Gray, H. B.; Siiman, O.; Grunthaner, F. J. *J. Am. Chem. Soc.* **1974**, *96*, 2644. (b) Papaefthymiou, V.; Millar, M. M.; Munck, E. *Inorg. Chem.* **1986**, *25*, 3010.
- (15) (a) Surerus, K. K.; Chen, M.; van der Zwaan, J. W.; Rusnak, F. M.; Kolk, M.; Duin, E. C.; Albracht, S. P. J.; Muenck, E. *Biochemistry* **1994**, *33*, 4980. (b) Christner, J. A.; Munck, E.; Janick, P. A.; Siegel, L. M. *J. Biol. Chem.* **1981**, *256*, 2098.
- (16) Gorman, C. B.; Smith, J. C.; Hager, M. W.; Parkhurst, B. L.; Sierzputowska-Gracz, H.; Haney, C. A. *J. Am. Chem. Soc.* **1999**, *121*, 9958.
- (17) Cambay, J.; Lane, R. W.; Wedd, A. G.; Johnson, R. W.; Holm, R. H. *Inorg. Chem.* **1977**, *16*, 2565.
- (18) Henderson, R. A. *Chem. Rev.* **2005**, *105*, 2365.
- (19) (a) Tezuka, M.; Yajima, T.; Tsuchiya, A.; Matsumoto, Y.; Uchida, Y.; Hidai, M. *J. Am. Chem. Soc.* **1982**, *104*, 6834. (b) Tomohiro, T.; Uoto, K.; Okuno, H. *J. Chem. Soc., Chem. Commun.* **1990**, 194.
- (20) Morandrea, A.; Fortage, J.; Edvinsson, T.; Le Pleux, L.; Blart, E.; Boschloo, G.; Hagfeldt, A.; Hammarström, L.; Odobel, F. *J. Phys. Chem. C* **2008**, *112*, 1721.